General and Comparative Endocrinology 282 (2019) 113218

Contents lists available at ScienceDirect

General and Comparative Endocrinology

journal homepage: www.elsevier.com/locate/ygcen

Subfertility and reduced progestin synthesis in Pgrmc2 knockout zebrafish

Xin-Jun Wu[a], Marcus Jermaul Williams[a], Pujan Rameshkumar Patel[a], Kimberly Ann Kew[b], Yong Zhu[a,*]

[a] Department of Biology, East Carolina University, Greenville, NC 27858, USA
[b] Department of Chemistry, East Carolina University, Greenville, NC 27858, USA

ARTICLE INFO

Keywords:
Pgrmc2
Subfertility
Progestin
Oocyte maturation
Steroid synthesis
DHP

ABSTRACT

Progestin receptor membrane component (Pgrmc1 & 2) is a heme-binding protein. Studies on Pgrmc1 have suggested possible roles in heme binding, activation of steroid-synthesizing P450s, along with binding and transferring of membrane proteins. However, the studies of Pgrmc1's paralog, Pgrmc2 are still lacking. In order to determine the physiologic function(s) of Pgrmc2, we generated a zebrafish mutant line (*pgrmc2*$^{-/-}$). We found a reduction in both spawning frequency and the number of embryos produced in female *pgrmc2*$^{-/-}$. This subfertility is caused by reduced oocyte maturation (germinal vesicle breakdown, GVBD) in *pgrmc2*$^{-/-}$ in vivo. Nonetheless, oocytes from *pgrmc2*$^{-/-}$ had similar sensitivity to 17α,20β-dihydroxy-4-pregnen-3-one (DHP, a maturation induced progestin in zebrafish) compared with wildtype (*wt*) in vitro. Therefore, we hypothesized that oocyte maturation tardiness found in vivo, could be due to lack of progestin in *pgrmc2*$^{-/-}$. Interestingly, we found significant reduced expression of hormones, receptors, and steroid synthesizing enzymes including *lhcgr*, *egfra*, *ar*, and *esr2*, *cyp11a1* and *hsd3b1*. In addition, DHP levels in *pgrmc2*$^{-/-}$ ovaries showed a significant decrease compared to those in *wt*. In summary, we have provided a plausible molecular mechanism for the physiological functions of Pgrmc2 in the regulation of female fertility, likely via regulation of receptors and steroids in the ovary, which in turn regulates oocyte maturation in zebrafish.

1. Introduction

Progestin receptor membrane component 1 (Pgrmc1) is a heme binding protein, which binds and regulates cytochrome P450 protein activities and affects steroid metabolism (Oda et al., 2011; Rohe et al., 2009; Szczesna-Skorupa and Kemper, 2011). Pgrmc1 has also been suggested as a P4 receptor, an adaptor protein transferring receptors to the cell membrane to mediate P4 signaling, or an regulator of gene and protein expression (Peluso, 2013; Thomas, 2008; Thomas et al., 2014; Wu et al., 2018; Zhu et al., 2008). In addition, PGRMC1 has also been suggested to mediate antiapoptotic and antimitotic actions of P4 in rat granulosa cells (Peluso et al., 2008). In contrast to studies conducted in Pgrmc1, studies on Pgrmc2 are rare.

Pgrmc2, like Pgrmc1, also contains a cytochrome b5 domain, indicating that Pgrmc2 may be able to bind heme and regulate cytochrome P450 proteins. Recent studies in PGRMC2 knockout mice have suggested that knocking out PGRMC2 causes premature reproductive senescence in female mice, possibly due to failure of implantation (Clark et al., 2016). However, the conserved functions of Pgrmc2 in non-mammalian vertebrates have not been studied. The effect of Pgrmc2 on reproductive processes such as oogenesis, steroid synthesis, fertility and underlying mechanisms in basal vertebrates is unclear.

In the present study, we generated a zebrafish mutant for Pgrmc2 and examined the functions of Pgrmc2 in reproduction. We found for the first time that Pgrmc2 regulated several receptors and steroid synthesis enzymes, which in turn regulate DHP, oocyte maturation and fertility in zebrafish.

2. Materials and methods

2.1. Animals

The Tübingen strain of zebrafish (*Danio rerio*) used here originated from the Zebrafish International Resource Center, and then were propagated in our lab following previously published guidelines (Zhu et al., 2015). Zebrafish were raised at 28.5 °C on a 14-h light, 10-h dark cycle, and were fed twice daily. All procedures were approved by the Institutional Animal Care and Use Committee (IACUC) at East Carolina University.

* Corresponding author at: Department of Biology, Howell Science Complex, East Carolina University, 1000 E. 5th Street, Greenville, NC 27858, USA.
E-mail address: zhuy@ecu.edu (Y. Zhu).

https://doi.org/10.1016/j.ygcen.2019.113218
Received 10 March 2019; Received in revised form 14 June 2019; Accepted 6 July 2019
Available online 10 July 2019

2.2. Design CRISPR-Cas9 targets and preparation of Cas9 mRNA and sgRNAs

A 5′GG-(N_{18})-NGG3′ target site in exon 1 of *pgrmc2* (GGGGCCGGT CTCGGTTTAGGCGG) was selected (Fig. 2). Cas9 mRNA and gRNA were synthesized using a modified protocol (Jao et al., 2013; Ran et al., 2013). For Cas9 transcripts (nls-zCas9-nls RNA), a template plasmid (pCS2-nls-zCas9-nls) was linearized by NotI digestion, and then purified using a QIAprep column (Qiagen, Germantown, MD, USA). Capped Cas9 mRNA (nls-zCas9-nls) was synthesized using mMACHINE SP6 kit (Fisher Scientific, Hampton, NH, USA) and purified using RNeasy Mini kit (Qiagen). For gRNA, template plasmids were linearized by BamHI digestion and purified using a QIAprep column. The gRNA was generated by in vitro transcription using MEGAshortscript T7 kit (Fisher Scientific). RNA concentration was quantified using a Nanodrop spectrophotometer (Nanodrop 2000, ThermoFisher). The size and quality of the resulting gRNA was confirmed by electrophoresis using a 2% (wt/vol) formaldehyde agarose gel.

2.3. Establishment Pgrmc2 mutant line

To generate a founder population (F0), fertilized eggs were collected from wildtype fish within 5 min of natural spawning in their crossing tanks, which were set up the night before. One-cell-stage embryos were injected using glass needles, and injection was driven by compressed N_2 gas, under the control of a PV820 Pneumatic PicPump (World Precision Instrument, Florida, USA). Approximately 100 ng/μl of gRNA, 150 ng/μl of Cas9 mRNA and 0.1% phenol red were co-injected into the yolks of the embryo using a glass microcapillary pipette attached to a micromanipulator under a stereomicroscope (Leica MZ6). To estimate mutagenesis efficiency, embryos without microinjection were designated as wildtype and used as the control group. The genomic DNA was extracted from 30 normally developing wildtype or CRISPR/Cas9-gRNA-microinjected embryos two-day post fertilization (dpf), using the HotSHOT method (Meeker et al., 2007). Mutation rates were estimated by comparing the band intensities of undigested PCR products, to the intensities of digested PCR products using T7 endonucleases I assay (Zhu et al., 2015). The PCR products were cleaned through a Qiagen column, cloned into a TA cloning vector, and potential mutant clones were selected for DNA sequencing analysis to confirm the presence of frame-shift mutation (Zhu et al., 2015).

To identify germline-transmitted mutations, remaining F0 founder embryos were raised to adulthood and outcrossed with wildtype fish. Genomic DNA from each cross was extracted from 30 randomly selected and pooled F1 embryos, and the status of the target site was analyzed via PCR amplification, T7 Endonucleases I assay, and DNA sequencing as described above. The remaining F1 embryos with identified frame shift mutations were raised to adulthood and were individually genotyped. Genomic DNA was extracted from part of the caudal fin of each adult fish in a 50 μl hot alkaline solution, then analyzed as stated above. Heterozygous F1 adults, that carried the same frameshift mutant alleles were crossed with each other. These crosses yielded wildtype, heterozygous, and homozygous F2 fish that were further genetically and physiologically characterized. A mutant-specific reverse primer was then designed according to the mutated sequence in CRISPR/Cas9-induced mutation (*pgrmc2*-Forward: 5′-TCAAAAGCCTTTGTTTGGTC-3′; *pgrmc2*-wildtype Reverse: 5′-GCAGCATGCCGCCTAAACC-3′; *pgrmc2*-mutant Reverse: 5′-AATCTGAGACTGAGCATGCCG-3′). PCR condition were then optimized for efficient identification of these specific mutations. After initial denaturation for 2 min at 94 °C, the cycling reaction was performed with the profile of 30 s at 94 °C, 30 s at 61 °C and 45 s at 72 °C for 35 cycles, followed by a 10-min extension at 72 °C with a Thermal Cycler (Eppendorf, Hauppauge, NY, USA).

Table 1
PCR primers used for real-time quantitative PCR (qPCR).

Name	Strand	Sequences (5′-3′)	Product size (bp)
ar	F	GGATGCTGTACTTCGCTCCA	224
	R	GTACGTCAGACGCAGCTCAT	
cyp11a1	F	TGCTTTTGCCGAAGTTGCAG	281
	R	GGGTAGGTACAGCATGGGTG	
cyp17a1	F	CAGCGACAGGGGGAATCTAC	356
	R	ACCTTTGCAAAATCCACGCC	
cyp19a1a	F	AAAGTTCAACTGGCACACGC	319
	R	CGACCGGGTGAAAACGTAGA	
egfra	F	GGACGACCGCATGCATTTAC	292
	R	AGGCTGAAAGTCTCCCTCCT	
esr1	F	CTGTGGCTCGATTTCGGAGT	281
	R	TGTGTGACTCTCAATGTACCTCA	
esr2a	F	CACTGGTAAAGCGGGTAGCA	495
	R	TGAGATAAATCTCCGGCGGC	
esr2b	F	TGCTCTCACACATCCGACAC	201
	R	TGTCTTTCAGGTCAGGCTGC	
fshb	F	GCGCAGAATCAGAATGCAGG	235
	R	GAATCAACCCCTGCAGGACA	
fshr	F	ATGGGAAACCAGCAGCTGAA	396
	R	GATGTCCTCGCAAGGGTTGA	
gapdhs	F	TGTGGTTGTGTCTGCTCCATC	217
	R	ATCGACAGTCTTCTGTGTGGC	
gnrh3	F	TTGCCAGCACTGGTCATACG	183
	R	TTCAGAGGCAAACCTTCAGCA	
gnrhr2	F	CACGACCTACGGCAGCTTTA	297
	R	AACCAGTACCACAGGCCAAG	
gnrhr4	F	ACAAGCGCAAGTCCCATGTA	192
	R	CCACGGTCACAAATGCACAG	
hmgcra	F	ATGACTAGAGGGCCAGTGGT	286
	R	TGAGTGACGGGGTTTCACAA	
hmgcrb	F	ACAAACCAAACCCCGTCACT	404
	R	CCGATCAGGTGCTTCCCTTT	
hsd3b1	F	AGCTTGCTGAGATCCGACTG	208
	R	AGTTCACTGTATTCAACTGCTCC	
hsd17b1	F	TGTGCATGTCTGATCTTTACGG	361
	R	CATAAGACCCACACCGGCAT	
insig1	F	GGACACGCTATTTTCGTCCG	228
	R	CTGTTAAGGATACAGCACTGGC	
igf1	F	AGAAGGTCACACAACCGTGG	223
	R	TGTTTCCTCGGCTCGAGTTC	
lhb	F	TTTCCACGCTGTGAGCTAGT	239
	R	GCCACCGGGTATGTGATCTG	
lhcgr	F	CGCTCTGATCAACTGGGACA	218
	R	GGCGCTGTTGGCATAAATCC	
paqr5a	F	TGCCAAAGACTGCGTGCTAA	281
	R	GGCTGTAGAAGCTGAGTGCT	
paqr5b	F	GCTTGGCTTACCATTGCTTCAC	223
	R	AAGGAATGCAAGCAGCGTATG	
paqr6	F	AAGCTCTGGCCAGTCATTCC	193
	R	CGGGACGCCATGTCTGATAA	
paqr7a	F	GTTGTCTGTCTTGCTTCGGC	243
	R	GTCCAGCGCGTTTTTCTTCA	
paqr7b	F	CGTACTTGTGAGTGCAAGGGT	165
	R	GAAACGAGGGATCTGGCGAA	
paqr8	F	TGCTCAGCGCTGTTACCAAG	372
	R	GCAGCTCGTTGTGACATTGG	
paqr9	F	GTCCCACCAATGAGACTGGG	277
	R	TACGCCAATGAGGAACCCAC	
pgrmc2	F	ACCAAGGTCTTCGACGTGAC	250
	R	ATGGTTCGTCTCCTGGCTTC	
star	F	TGTAAGGGCTGAGAATGG	220
	R	TCAGCAAGCAATGGCTGC	

2.4. Spawning and fertility

After all zebrafish lines reached their maturity at ~4-months of age, at least 10 homozygous mutant female fish were crossed with wildtype fertility confirmed males. Production of the offspring for each genotype was recorded daily for a period of two weeks, following a two-week acclimation period. Spawning frequency is defined as the number of times a female would produce fertilized embryos in a two-week examination period.

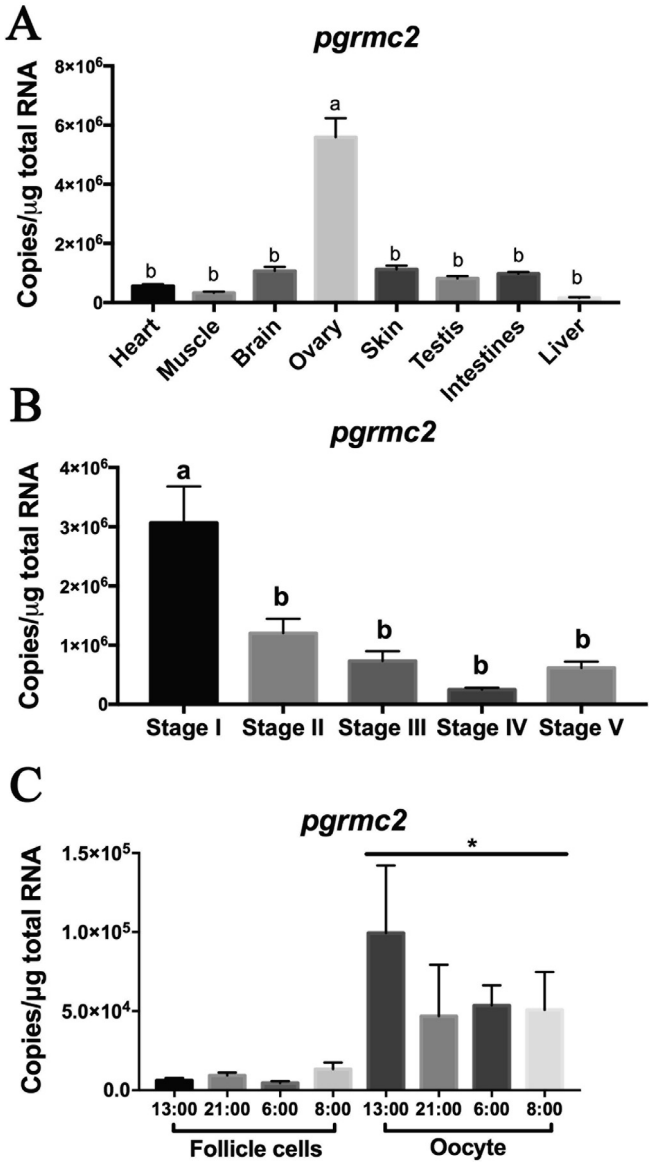

Fig. 1. Expression of *pgrmc2* transcripts in zebrafish. (A) Expression of *pgrmc2* in various tissue types, with the highest expression level seen in the ovary. (B) Expression of *pgrmc2* in different follicle stages. Stage I oocytes showed highest *pgrmc2* expression. (C) Expression of *pgrmc2* in follicular cells and denuded oocytes. Bars with different letters indicated significant difference. Significant difference was observed between follicle cells and denuded oocytes. *, $p < 0.05$.

2.5. Yolk width measurement

In total, 7 individuals of *wt* or *pgrmc2*$^{-/-}$ female fish were used and paired with wildtype males. Width of the yolk was defined as the length between two tips of the yolk. All embryos (~100 embryos/pair) from each pair were collected in a petri dish and the diameter of the yolks was measured and recorded using a stereo microscope (SZX7, Olympus, Japan). To reduce variation, yolk width was determined at 30% epiboly stage.

2.6. Follicle isolation and quantification

Oocyte maturation in zebrafish typically occurs prior to the onset of (day) light, while ovulation and spawning occurs within 1 h following the onset of light. At 09:30 AM, thirty minutes after laboratory lights were turned on, seven adult female fish were placed in a lethal dose of MS-222 (300 mg/L buffered solution) for 10 min, and then the spinal cord and blood supply was severed using IACUC approved procedures. The ovaries of each fish were then immediately dissected out and rinsed in 60% L-15 media (Sigma-Aldrich, St. Louis, MO, USA) containing 15 mM HEPES (pH = 7.2). The term "follicles" refers to follicular cell enclosed oocytes. Follicles of various sizes were isolated from the ovaries and the diameter of each follicle was measured under a stereo microscope (SZX7, Olympus, Japan). The developmental stages of follicles were divided into five different stages based on follicular size, morphological criteria, physiological and biochemical characteristics (Selman et al., 1993; Tyler and Sumpter, 1996) with a slight modification. Stage I (< 140 μm) and II (140–340 μm) follicles are previtellogenic follicles; Stage III are early vitellogenic follicles (340–690 μm); Stage IV are late vitellogenic follicles (690–730 μm) that are further divided into IVa and IVb two stages, IVa is maturational competent fully grown but immature follicles (IVa), IVb are matured follicles that undergo oocyte maturation but haven't undergone ovulation (IVb); and Stage V ovulated follicles are ovulated eggs with no follicular cells attached (730–750 μm).

2.7. Oocyte maturation assay

Ovarian follicles were isolated and incubated in order to determine the sensitivities of follicles to a maturation inducing steroid, DHP (Hanna and Zhu, 2011; Pang and Thomas, 2009). Gravid female zebrafish were euthanized and their ovaries were immediately dissected out. Then, the ovaries were washed several times in 60% L-15 medium (Sigma-Aldrich). The individual ovarian follicles were carefully separated without damaging the follicular cell layers based on previously established protocols (Hanna and Zhu, 2011). Fully grown immature oocytes were randomly selected and distributed into the wells of a 24-well plate (~30 follicles/well). Final concentration for DHP and ethanol in the treatment group was 5 nM and 0.1%, respectively. As a control, 1 μl pure ethanol was added into control wells containing 1 ml medium and same number of follicles (~30 follicles/well) collected at the same time from the same group of individual fish. The follicles were incubated in vehicle or DHP for 5 h, with GVBDs being scored every half hour during the incubation period. In order to confirm the results, all the experiments were repeated five times.

2.8. RNA isolation and real-time quantitative PCR

Brain, liver, and ovary tissues were quickly dissected out of mature fish around 5:30am prior to oocyte maturation and homogenized immediately in 500 μl of RNAzol reagent (Molecular Research Center, Cincinnati, OH, USA). The homogenized samples were preserved in −80 °C freezer until RNA extraction. Total RNA was isolated based on a modified protocol (Liu et al., 2017). The amount and purity of the RNA was determined using a Nanodrop 2000 (Thermo Fisher). The cDNAs were synthesized using 500 ng total RNA and High Capacity cDNA Reverse Transcription kit (Thermo Fisher). Real-time quantitative PCR (qPCR) was performed using the SYBR green with C1000 Touch Thermal Cycler (Bio-Rad). The protocol consisted of a cycling profile of 30 s at 95 °C, 30 s at 58 °C, and 45 s at 72 °C for 45 cycles followed by a melting curve test. PCR efficiency was calculated using the efficiency equation (EFF) = 10(−1/slope) − 1, and the authentic PCR products were confirmed by analyses of melting curve, gel electrophoresis, and DNA sequencing. Because the expressions of house-keeping-gene were variable in different developmental stages of oocytes, we determined *pgrmc2* transcript by the absolute transcript. The *pgrmc2* transcript was determined using Ct-values of samples and standard curves generated from known serial diluted plasmid concentrations (10^2–10^7 copies/μL). We used the comparative Ct method for various gene expression in brains, livers and ovaries, and the data was normalized using *gapdhs* and expressed as fold differences of target gene expression in *pgrmc2*$^{-/-}$ relative to those in the wildtype control. The full names of the genes

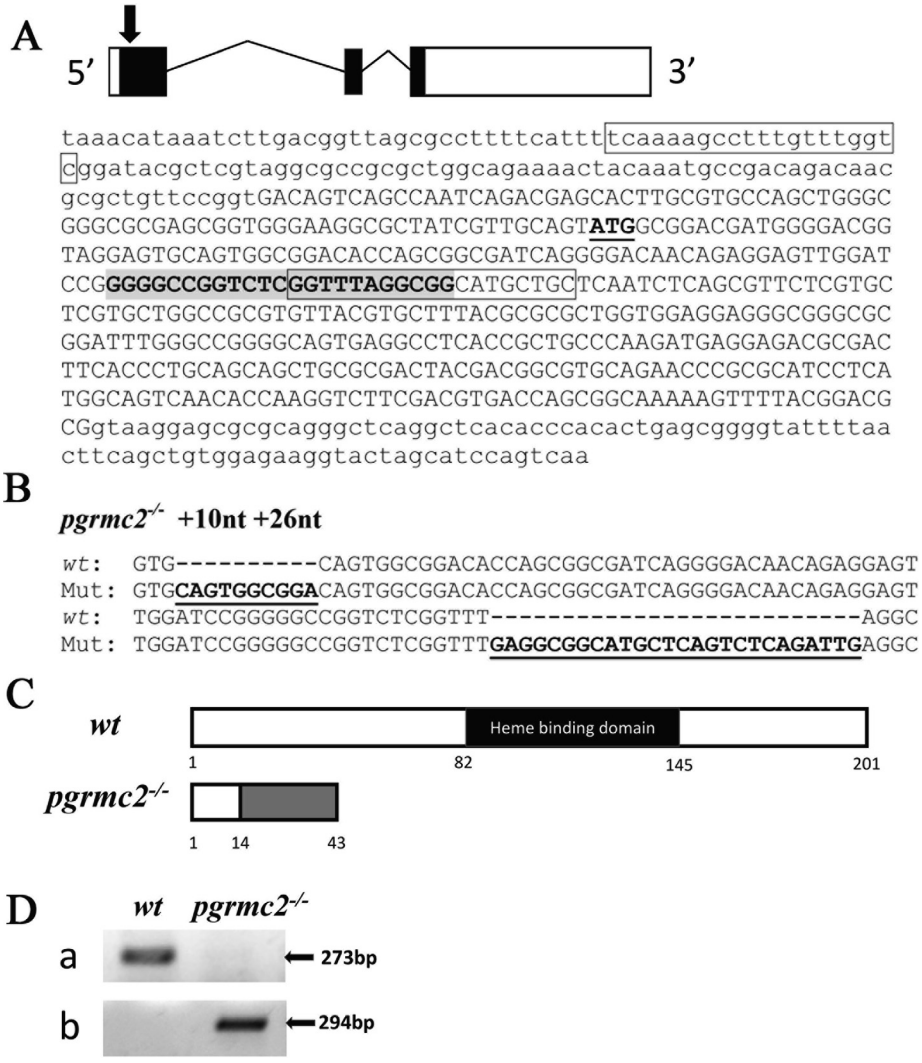

Fig. 2. Targeted and heritable genetic modification of zebrafish progesterone receptor membrane component 2 (*pgrmc2*) gene. (A) Organization of three exons and two introns for *pgrmc2* and the CRISPR/Cas9 target site. Exons are indicated by boxes; introns are indicated by black lines. Coding exons are labeled with filled black box, while untranslated regions are labeled with open box. Approximate location of the CRISPR/Cas9 target in exon 1 of pgrmc2 is indicated by a downward black arrow. In addition, genomic DNA sequence of first exon (in upper case) and flanking intron regions (in lower case) of Pgrmc2 are shown. Translation start sites (ATG) are indicated by bolded and underlined font. The sequence highlighted in grey is the CRISPR/Cas9 target site with a PAM motif (CGG). Location of PCR primers for distinguishing the mutant from the wildtype is indicated with two open boxes. (B) Comparison of mutant genomic DNA sequences (small insertions) in *pgrmc2*$^{-/-}$ to those in wildtype (*wt*). Modified sequence regions are bolded and underlined. (C) Schematic drawings show wildtype Pgrmc2 protein and predicate truncated proteins from *pgrmc2*$^{-/-}$ lacking heme binding domains. Small insertions in the pgrmc2 coding region, resulting in a premature stop codon in the Pgrmc2 protein. (D) Gel images of PCR products using a Pgrmc2 wildtype specific primer (a), or a Pgrmc2 mutant specific primer (b) to distinguish *pgrmc2*$^{-/-}$ from wildtype fish.

and the primers used in this study are listed in Table 1.

2.9. To determine DHP in the ovaries

Ovaries were collected from 4-month old healthy and mature *wt* or *pgrmc2*$^{-/-}$ at 5:30 am prior to oocyte maturation. Immediately, collected ovaries were sonicated (Sonic Dismembrator, Fisher Scientific) in 600 µl of optima grade water (Fisher Scientific, Fairlawn, NJ) on ice. Samples were then stored in −80 °C until the analysis. Steroids were extracted from the samples using a liquid–liquid extraction (LLE) method. Briefly, 2.4 ml extraction solvent (methanol: water in 1:1 ratio containing 0.1% formic acid) was added to each sample and vortexed for 5 min. The mixture was centrifuged for 15 min at 14,000 *g*, and the supernatant (organic phase) was transferred into a 16 × 125mm borosilicate glass tube (VWR, Radnor, PA). Then, 3 ml of methyl-*tert*-butyl-ether (Fisher Scientific) was added to the supernatant. The mixture was vortexed for 15 min and centrifuged for two minutes at 800 *g*. The organic phases on the top was collected. The extraction process was repeated twice in the remaining aqueous phase. The collected organic fractions from three ovarian samples were combined in the same tube, and was dried with N_2 gas at a room temperature. Each sample was resuspended in 100 µl of sample buffer (70 acetonitrile:30 water containing 0.1% formic acid) for liquid chromatography/mass spectrometry (LCMS) analysis.

To determine the DHP level in samples, an external standard calibration curve was established using a serial of known concentration (0.005, 0.01, 0.05, 0.1, 0.5 µg/ml) of 17α,20β-dihydroxy-4-pregnen-3-one (DHP, Sigma-Aldrich, St. Louis, Missouri). Extracted steroids were identified using an Eskigent 425 microLC/SCIEX 5600 + Triple time-of-flight mass spectrometer. Samples and standards in autosampler vials were loaded in a refrigerated holder (4 °C). A HALO C18, 2.7 µm, 0.5 × 50 mm microLC column purchased from Eksigent was maintained at 25 °C. The flow rate was 10 µl/min and 5 µl of sample was injected. Mobile phase A: water with 0.1% formic acid and mobile phase B: acetonitrile. Independent data acquisition was utilized to collect the top 20 MS/MS. For data quantification, the integration of peak areas was conducted using PeakView and MultiQuant (SCIEX), and an external standard calibration curve was used to calculate the DHP amount and normalized by the ovary weight.

2.10. Statistical analysis

All graphs were generated and results were analyzed using GraphPad Prism 7.0a (San Diego, CA, US). Significant differences among paired treatment groups were determined using Student's *t*-test with a significance level of $p < 0.05$. Gene expressions at different stage of oocytes and in different tissues were analyzed by one-way analysis of variance (ANOVA), followed by Tukey's multiple comparisons test. A paired *t*-test was used to compare the differences between follicular cells and denuded oocytes across different time points.

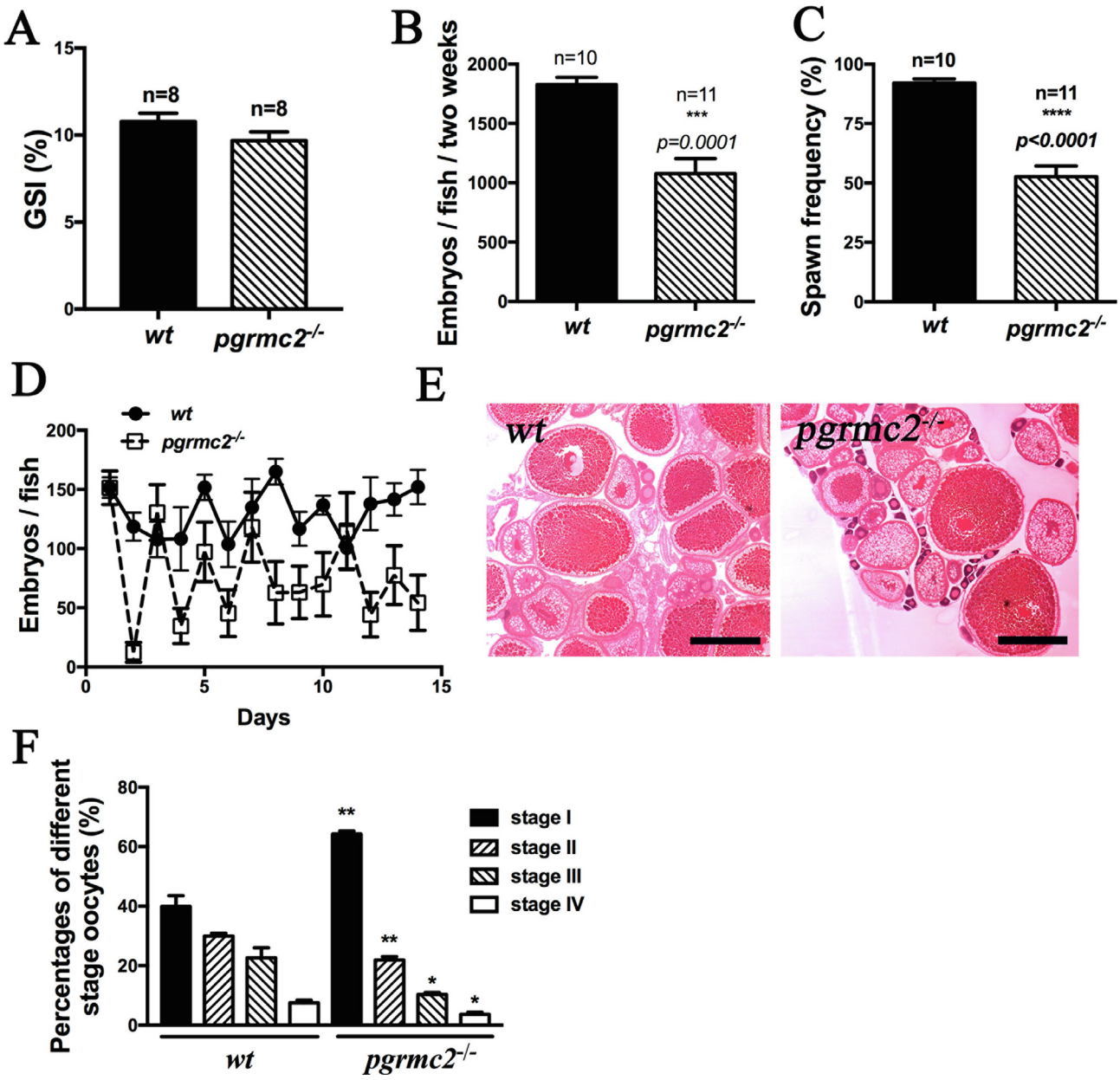

Fig. 3. Comparison of ovarian size, fertility and morphology between *pgrmc2*$^{-/-}$ and wildtype. (A) Comparison of ovarian size, gonadosomatic index (GSI) between *pgrmc2*$^{-/-}$ and wildtype. (B) Mutant *pgrmc2*$^{-/-}$ female zebrafish produced fewer embryos over a 2-week mating period. (C) Mutant *pgrmc2*$^{-/-}$ female zebrafish spawned with less frequency during the mating period. (D) Mutant females produced fewer embryos daily than wildtype females. (E) Morphology comparison of the ovaries. HE staining of a representative ovarian section from a *pgrmc2*$^{-/-}$ female showed well-formed different stages of oocytes with a significantly higher number of Stage I follicles compared to wildtype. Scale bars: 500 μm. (F) A higher number of Stage I follicles, but a lower number of late stage follicles were observed in *pgrmc2*$^{-/-}$ compared to wildtype. $^{*}p < 0.05$; $^{**}p < 0.01$; $^{***}p < 0.001$; $^{****}p < 0.0001$.

3. Results

3.1. High expression of pgrmc2 in ovary and Stage I follicles

Expression of *pgrmc2* was found in all examined tissues, including all reproductive tissues and all developmental stages of follicles, with highest expression of *pgrmc2* observed in the ovaries and Stage I follicles (Fig. 1A and 1B). In the follicles, *pgrmc2* is more highly expressed in denuded oocytes than in follicular cells (Fig. 1C).

3.2. Establishment of Pgrmc2 mutant line in zebrafish

To investigate Pgrmc2's functions in vivo, we targeted the first exon of Pgrmc2 as it contains the proper parameters for CRISPR/Cas9 target design (Fig. 2A). Successful editing was confirmed by Sanger sequencing. One mutant line had 10- and 20-nucleotide insertions in two different loci of Pgrmc2, which caused a translational frameshift in *pgrmc2* mRNA and an early stop codon, resulting in a truncated protein (Fig. 2B and 2C). CRISPR/Cas9-gRNA induced specific insertions effectively disrupting the translation of Pgrmc2 and led to the loss of heme binding domain (Fig. 2C). Using specific primers that target a frameshift site, we were able to easily differentiate *pgrmc2*$^{-/-}$ from wildtype using PCR (Fig. 2D).

3.3. Reduced fertility in pgrmc2$^{-/-}$ female zebrafish

No significant difference in ovarian size was observed in *pgrmc2*$^{-/-}$ females compared with their wildtype siblings (Fig. 3A). To evaluate

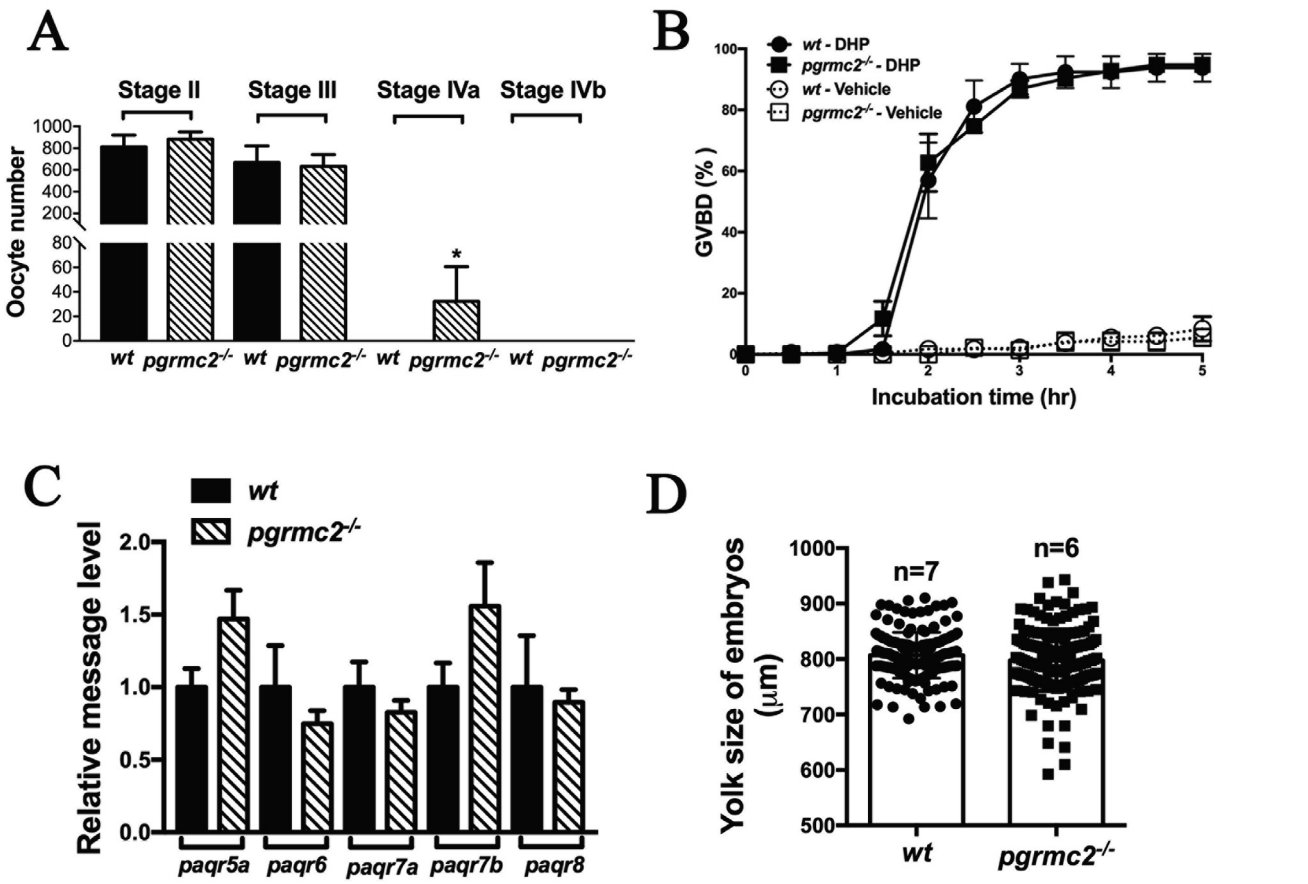

Fig. 4. Attenuation of oocyte maturation in vivo but not in vitro in *pgrmc2*$^{-/-}$. (A) Some leftover immature Stage IVa oocytes were observed in *pgrmc2*$^{-/-}$ 30 min after room lights were switched on, while no Stage IVa remained in *wt*, because all of them had matured and ovulated before lights were switched on that morning. There was no difference in terms of Stage II and Stage III oocyte number. (B) Similar sensitivity and oocyte maturation in response to progestin (DHP, 17α,20β-dihydroxy-4-pregnen-3-one) stimulation in vitro in fully-grown immature follicles from *pgrmc2*$^{-/-}$. (C) No difference of transcript of mPRs in Stage IVa follicles in *pgrmc2*$^{-/-}$ compared to *wt*. (D) Similar yolk sizes were observed in *pgrmc2*$^{-/-}$ embryos in comparison to those from *wt*. *, $p < 0.05$.

the fertility in mutant zebrafish, mature *pgrmc2*$^{-/-}$ females (n = 11) at 4 months of age, were mated with known fertile wildtype males during a minimum 4-week mating study period. The embryo numbers were recorded daily for two weeks and compared to those in wildtype crossing (wildtype males crossed with wildtype females, n = 10) following a two-week adaptation period. Interestingly, we found that *pgrmc2*$^{-/-}$ females (n = 11, 1077 ± 127.2 embryos/fish/two weeks, *p = 0.0001*) produced a significantly lower number of embryos in comparison with wildtype females (n = 10, 1827 ± 63.2 embryos/fish/two weeks) (Fig. 3B). The *pgrmc2*$^{-/-}$ females also spawned significantly less frequently (n = 11, 52.6 ± 4.65%) than wildtype females (n = 10, 92.14 ± 1.67%) (Fig. 3C). Overall, wildtype females produced more embryos daily than *pgrmc2*$^{-/-}$ females over two weeks of continuous mating tests (Fig. 3D). Histology analysis showed *pgrmc2*$^{-/-}$ ovaries have all stages of oocytes with a significantly higher percentage of Stage I follicles compared to that of wildtype (Fig. 3E and 3F). The high ratio of Stage I oocytes skewed the over proportions and resulted in lower percentages of late stage follicles in *pgrmc2*$^{-/-}$ compared to wildtype (Fig. 3F).

3.4. Maturation tardiness in vivo but not in vitro in *pgrmc2*$^{-/-}$

One possible cause for the reduced fertility found in *pgrmc2*$^{-/-}$ is deficiencies in oogenesis. We sampled ovaries 30 min after the lights turned on and counted the numbers of follicles in different stages. No significant differences were found in the number of early stage follicles (Stage II and Stage III) in the ovaries from *pgrmc2*$^{-/-}$ females compared to wildtype (Fig. 4A). Typically, fully grown immature follicles (Stage IVa) would have already successfully completed the processes of oocyte maturation and ovulation. As expected, no Stage IVa was observed in the ovaries from wildtype females (Fig. 4A). However, a significant number of Stage IVa follicles could still be observed in the *pgrmc2*$^{-/-}$ females (Fig. 4A). These results suggest reduced oocyte maturation in *pgrmc2*$^{-/-}$ in vivo.

One possible cause for reduced oocyte maturation is reduced progestin sensitivity due to reduced expressions of membrane progestin receptors. However, we surprisingly found that fully grown but immature follicles from *pgrmc2*$^{-/-}$ had normal sensitivity to DHP (Fig. 4B), as compared to those from wildtype females. Oocytes from *pgrmc2*$^{-/-}$ matured at the same rate as wildtype over the 5 h DHP treatment. In addition, no significant differences were found between wildtype and *pgrmc2*$^{-/-}$ in the expression of maturation related genes including *mprγ* (*Paqr5a*), *mprδ* (*paqr6*), *mpra1* (*paqr7a*), *mpra2* (*paqr7b*), and *mprβ* (*paqr8*) in the ovaries (Fig. 4C). Expressions of *mprγ2* (*paqr5b*) and *mpr⩽* (*paqr9*) were under qPCR detection limit (in 45 cycles) in Stage IVa follicles from wildtype and *pgrmc2*$^{-/-}$. The yolk sizes of 30% epiboly stage embryos were also measured. The mean yolk size of *pgrmc2*$^{-/-}$ embryos was similar to that of wildtype individuals (Fig. 4D). However, *pgrmc2*$^{-/-}$ had a large number of extremely small sized embryos (< 600 μm), all of which died by 4 days post fertilization. These results indicated that, the attenuated oocyte maturation found in vivo was not due to down-regulation of membrane progestin receptors in the Stage IVa follicles of *pgrmc2*$^{-/-}$.

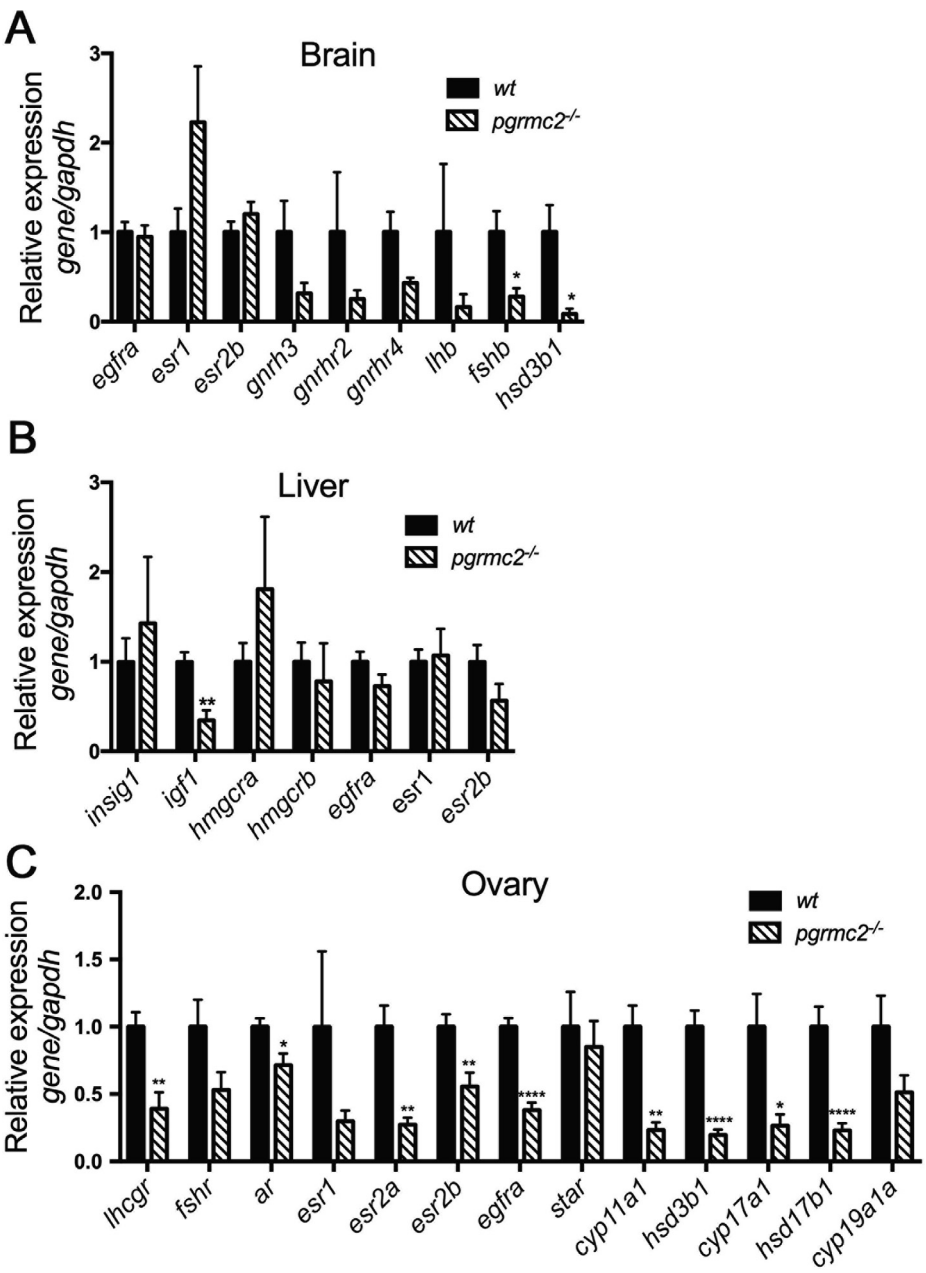

Fig. 5. Gene expression difference between wildtype and *pgrmc2*$^{-/-}$ females in brain (A), liver (B), and ovary (C). (A) In brain, *fshb* and *hsd3b1* are downregulated. (B) *igf1* is lower in liver of *pgrmc2*$^{-/-}$ and the genes involved in cholesterol synthesis show no change. (C) In the ovary, many genes express less in the *pgrmc2*$^{-/-}$, especially the steroid-synthesis enzymes. (*ar*: androgen receptor; *cyp11a1*: cytochrome P450 side-chain cleavage; *cyp17a1*: cytochrome P450 family 17 subfamily A member 1; *cyp19a1a*: cytochrome P450, family 19, subfamily A, polypeptide 1a; *egfra*: epidermal growth factor receptor a; *esr*: estrogen receptor; *fshb*: follicle stimulating hormone subunit beta; *fshr*: follicle stimulating hormone receptor; *gnrh*: gonadotropin-releasing hormone; *gnrhr*: gonadotropin-releasing hormone receptor; *hmgcr*: 3-hydroxy-3-methylglutaryl-CoA reductase; *hsd3b1*: 3β-hydroxysteroid dehydrogenase; *hsd17b1*: 17β-hydroxysteroid dehydrogenase; *igf1*: insulin-like growth factor 1; *insig1*: insulin induced gene 1; *lhb*: luteinizing hormone beta; *lhcgr*: luteinizing hormone receptor; *star*: steroidogenic acute regulatory protein).

3.5. Downregulation of genes that are essential for progestin synthesis

Thereafter, we hypothesized that reduced oocyte maturation in vivo is due to reduced progestin synthesis. In *pgrmc2*$^{-/-}$ adult female brains, follicle stimulating hormone subunit beta (*fshb*) and 3β-hydroxysteroid dehydrogenase (*hsd3b1*) were downregulated (Fig. 5A). In liver, the gene expression of the insulin-like growth factor 1 (*igf1*) was significantly lower in *pgrmc2*$^{-/-}$ than *igf1* expression in wildtype (Fig. 5B). Other genes that are important for cholesterol synthesis were expressed similarly to those in wildtype in the liver. Interestingly, significant down-regulation of steroidogenic enzymes including *cyp11a*, *hsd3b1*, *cyp17a1*, and *hsd17b1* were observed in the *pgrmc2*$^{-/-}$ ovaries. The *cyp11a* and *hsd3b1* are both essential for progesterone synthesis while *cyp17a1* and *hsd17b1* are important for testosterone and estradiol synthesis (Fig. 6). In addition, low expression of luteinizing hormone-choriogonadotropin receptor (*lhcgr*), androgen receptor (*ar*), estrogen receptor 2 (*esr2*, including *esr2a* and *esr2b*), epidermal growth factor receptor a (*egfra*) were also observed in the *pgrmc2*$^{-/-}$ ovaries.

3.6. Reduced progestin in pgrmc2$^{-/-}$ ovaries

To further elucidate why oocyte maturation delay happened in vivo but not in vitro in the ovaries of *pgrmc2*$^{-/-}$, we analyzed the progestin (DHP) content in ovaries using LCMS. As expected, the DHP level in the ovaries from *pgrmc2*$^{-/-}$ (0.076 ± 0.016 μg/g ovary, n = 4) was significantly lower than that in wildtype (0.30 ± 0.04 μg/g ovary, n = 4) ($p < 0.01$) (Fig. 7).

4. Discussion

Our previous report showed that *pgrmc1* regulates female fertility via regulation of mPRα and oocyte maturation (Wu et al., 2018). Pgrmc1 did not regulate oocyte maturation directly, but it facilitates plasma localization and expression of mPRα, which in turn indirectly regulates oocyte maturation (Thomas et al., 2014; Thomas et al., 2007; Wu et al., 2018). We also found that oocyte maturation was delayed in *pgrmc2*$^{-/-}$ in vivo. Unexpectedly, the oocyte maturation rate (GVBD) in vitro was similar in *pgrmc2*$^{-/-}$ compared to those in wildtype

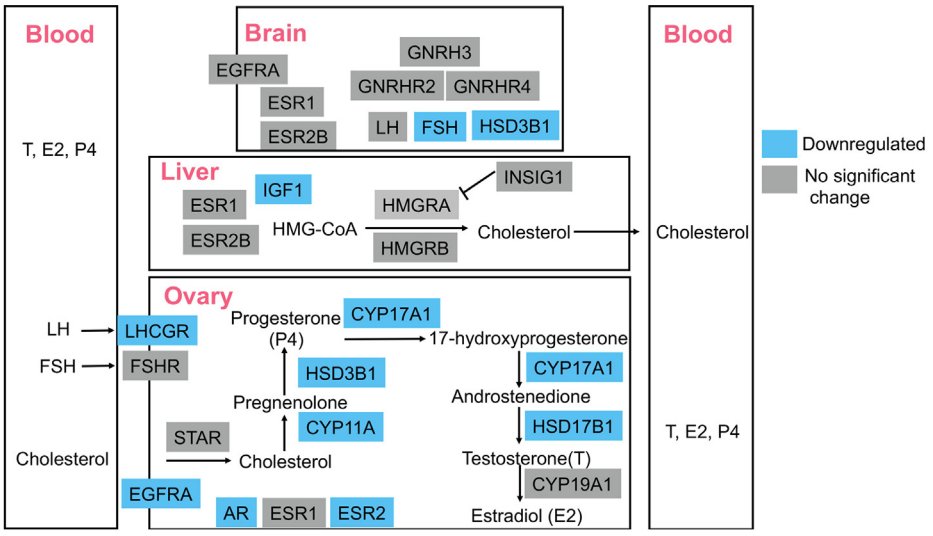

Fig. 6. Reproduction-related gene expressions in adult *pgrmc2*$^{-/-}$ female zebrafish in comparison to those in wildtype along the brain-liver-gonad axis. Using expression in the wildtype as reference, significantly down-regulated genes are marked in blue; genes with no statistically significant change are marked in grey. (*ar*: androgen receptor; *cyp11a1*: cytochrome P450 side-chain cleavage; *cyp17a1*: cytochrome P450 family 17 subfamily A member 1; *cyp19a1a*: cytochrome P450, family 19, subfamily A, polypeptide 1a; *egfra*: epidermal growth factor receptor a; *esr*: estrogen receptor; *fshb*: follicle stimulating hormone subunit beta; *fshr*: follicle stimulating hormone receptor; *gnrh*: gonadotropin-releasing hormone; *gnrhr*: gonadotropin-releasing hormone receptor; *hmgcr*: 3-hydroxy-3-methylglutaryl-CoA reductase; *hsd3b1*: 3β-hydroxysteroid dehydrogenase; *hsd17b1*: 17β-hydroxysteroid dehydrogenase; *igf1*: insulin-like growth factor 1; *insig1*: insulin induced gene 1; *lhb*: luteinizing hormone beta; *lhcgr*: luteinizing hormone receptor; *star*: steroidogenic acute regulatory protein).

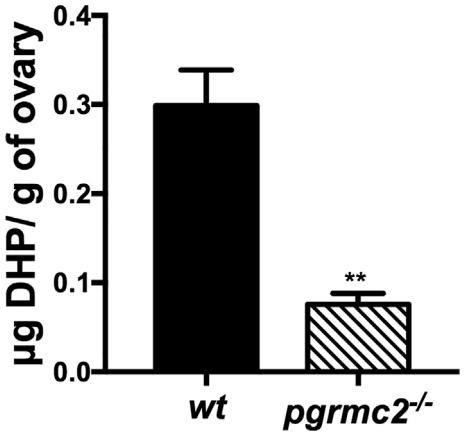

Fig. 7. Significant low level of 17α,20β-dihydroxy-4-pregnene-3-one (DHP) was found in *pgrmc2*$^{-/-}$ ovaries in comparison to those in wildtype (*wt*). The DHP values were determined using LC-MS. The results were shown as average (mean ± SEM) of four individual samples from wildtype or *pgrmc2*$^{-/-}$ ovaries. Each sample was pooled ovaries from three different individuals.

zebrafish. Furthermore, the expression of *mprs* in *pgrmc2*$^{-/-}$ was comparable to those in wildtype individuals. Therefore, the oocyte maturation tardiness found in *pgrmc2*$^{-/-}$ in vivo, was not caused by reduced sensitivity of progestin and mPRs expression in the oocytes in the *pgrmc2*$^{-/-}$. This deficiency is likely caused by lower progestin synthesis level found in *pgrmc2*$^{-/-}$ ovaries. We also found that *pgrmc2* expressed was relatively high in the oocytes and fluctuated during spawning. It is possible that Pgrmc2 has a role in trafficking membrane proteins including mPR α to the oocyte surface, and this role of Pgrmc2 may be compensated by Pgrmc1 in *pgrmc2*$^{-/-}$.

Previous studies demonstrated that PGRMC1 binds cytochrome P450(CYP) proteins: CYP51, CYP21A2, CYP21, CYP7A1 and CYP3A4 and alters the activities of these proteins (Hughes et al., 2007). The conservation of cytochrome b5 heme binding domain among Pgrmc1 and Pgrmc2 suggest Pgrmc2 may also has a role in steroid synthesis (Cahill, 2007). The expressions of several steroidogenesis enzymes were downregulated in our *pgrmc2*$^{-/-}$. CYP11A1 is a mitochondrial enzyme that catalyzes the conversion of cholesterol to pregnenolone, the first and rate-limiting step in the synthesis of the steroid hormones. HSD3B1 catalyzes the biosynthesis of progesterone from pregnenolone. Reduced expression of *cyp11a1* and *hsd3b1* and in *pgrmc2*$^{-/-}$ ovaries likely leads to reduced steroid synthesis including progestin, which causes oocyte maturation tardiness in *pgrmc2*$^{-/-}$. The expression level of *hsd17b1* is also lower in the *pgrmc2*$^{-/-}$. This enzyme is responsible for the interconversion of estrone (E1) and estradiol (E2), and for the interconversion of androstenedione and testosterone. Only one previous study suggested that PGRMC2 might have a role in steroid synthesis. Albrecht and colleagues showed PGRMC2 was detected in the endoplasmic reticulum (ER) in SKOV-3 cells, and PGRMC2 interacts with both the cytochrome P450 proteins CYP21A2 and CYP3A4 in HEK293T cells (Albrecht et al., 2012). Since CYP21A2 plays an important role in steroidogenesis and CYP3A4 in bile acid synthesis (DeBose-Boyd, 2007), Albrecht et al suggested PGRMC2 might be involved in cholesterol metabolism pathways like bile acid synthesis and steroidogenesis (Albrecht et al., 2012). To our knowledge, this is the first evidence of Pgrmc2 in steroidogenesis in an animal model in vivo. However, further studies are required to understand the underlying mechanisms of Pgrmc2 in the regulation of steroid synthesis.

To date, the identities of nongenomic progestin receptors in meiosis resumption and oocyte maturation are still the subject of hot debate. Pgrmc2 is unlikely the membrane progestin receptor that is essential for meiosis resumption and oocyte maturation process, though Pgrmc1 and Pgrmc2 have been suggested to be the membrane progestin receptors (McCallum et al., 2016; Peluso, et al., 2014). This hypothesis is supported by our results, i.e., oocytes from *pgrmc2*$^{-/-}$ has similar sensitivity to progestin as oocytes from wildtype. To our knowledge, there is no study that indicates Pgrmc2 binds progestins with high affinity. In addition, PGRMC2 siRNA treatment does not reduce the binding capacity of spontaneously immortalized rat granulosa cells (SIGCs) to P4 (Peluso et al., 2014). However, studies about Pgrmc2 are very limited, more studies are required to understand the roles of Pgrmc2 in steroid synthesis and oocyte maturation.

Both Pgrmc1 and Pgrmc2 are important for the female fertility. Reduced-fertility phenotypes were found in both *pgrmc1*$^{-/-}$ and *pgrmc2*$^{-/-}$ zebrafish, and also in the PGRMC1 and PGRMC2 conditional knockout mice (Clark et al., 2016; McCallum et al., 2016). Besides the delay of oocyte maturation in Pgrmc mutant zebrafish, a higher percentage of Stage I oocytes also were found in *pgrmc1*$^{-/-}$ and *pgrmc2*$^{-/-}$ females than in wildtype, which may suggest a role of Pgrmc2 in early oogenesis by regulating expression of other surface receptors such as Fshr. The Fshr knockout leads to failure of follicle activation with all ovarian follicles arrested at the primary growth-previtellogenic transition in female zebrafish (Zhang et al., 2015). Lower expression of *fshb* and *lhcgr* in *pgrmc2*$^{-/-}$ may also likely contribute to a deficit in follicle growth and a higher percentage of Stage I

oocytes. This may also contribute to the reduced fertility found in *pgrmc2*$^{-/-}$ females.

In summary, we found that Pgrmc2 has roles in fertility and in steroid synthesis by regulating expressions of steroid synthesizing enzymes. The Pgrmc2 mutation lead to reduced progestin syntheses, which can cause oocyte maturation tardiness in vivo. However, further studies are required to elucidate molecular mechanisms underlying the actions of Pgrmc2.

Author contribution

Y.Z. conceived the project and generated knockouts. X.W. and Y.Z. designed the experiments, performed the experiments and analyzed the data, and wrote the manuscript. M.J.W. conducted the qPCR experiments and wrote the manuscript. P.R.P and K.A.K. did liquid–liquid extraction and LCMS.

Funding

This work was supported by the NIH GM100461.

Declaration of Competing Interest

The authors have declared that no competing interests exist.

Acknowledgements

We want to thank Mr. Christopher M. Anderson for proof reading, Miss. Tara Dunn for her assistance in sectioning and analyses of ovarian samples, and Dr. Thomas Fink for his assistance in photographing and microscopic analyses.

References

Albrecht, C., Huck, V., Wehling, M., Wendler, A., 2012. In vitro inhibition of SKOV-3 cell migration as a distinctive feature of progesterone receptor membrane component type 2 versus type 1. Steroids 77, 1543–1550.

Cahill, M.A., 2007. Progesterone receptor membrane component 1: an integrative review. J. Steroid Biochem. Mol. Biol. 105, 16–36.

Clark, N.C., Pru, C.A., Yee, S.-P., Lydon, J.P., Peluso, J.J., Pru, J.K., 2016. Conditional ablation of progesterone receptor membrane component 2 causes female premature reproductive senescence. Endocrinology 158, 640–651.

DeBose-Boyd, R.A., 2007. A helping hand for cytochrome p450 enzymes. Cell Metab. 5, 81–83.

Hanna, R.N., Zhu, Y., 2011. Controls of meiotic signaling by membrane or nuclear progestin receptor in zebrafish follicle-enclosed oocytes. Mol. Cell. Endocrinol. 337, 80–88.

Hughes, A.L., Powell, D.W., Bard, M., Eckstein, J., Barbuch, R., Link, A.J., Espenshade, P.J., 2007. Dap1/PGRMC1 binds and regulates cytochrome P450 enzymes. Cell Metab. 5, 143–149.

Jao, L.-E., Wente, S.R., Chen, W., 2013. Efficient multiplex biallelic zebrafish genome editing using a CRISPR nuclease system. Proc. Natl. Acad. Sci. 110, 13904–13909.

Liu, D.T., Brewer, M.S., Chen, S., Hong, W., Zhu, Y., 2017. Transcriptomic signatures for ovulation in vertebrates. Gen. Comp. Endocrinol. 247, 74–86.

McCallum, M.L., Pru, C.A., Niikura, Y., Yee, S.-P., Lydon, J.P., Peluso, J.J., Pru, J.K., 2016. Conditional ablation of progesterone receptor membrane component 1 results in subfertility in the female and development of endometrial cysts. Endocrinology 157, 3309–3319.

Meeker, N.D., Hutchinson, S.A., Ho, L., Trede, N.S., 2007. Method for isolation of PCR-ready genomic DNA from zebrafish tissues. Biotechniques 43, 610.

Oda, S., Nakajima, M., Toyoda, Y., Fukami, T., Yokoi, T., 2011. Progesterone receptor membrane component 1 modulates human cytochrome P450 activities in an isoform-dependent manner. Drug Metabol. Dispos dmd.111.040907.

Pang, Y., Thomas, P., 2009. Involvement of estradiol-17β and its membrane receptor, G protein coupled receptor 30 (GPR30) in regulation of oocyte maturation in zebrafish, Danio rario. Gen. Comp. Endocrinol. 161, 58–61.

Peluso, J.J., 2013. Progesterone receptor membrane component 1 and its role in ovarian follicle growth. Front. Neurosci. 7, 99.

Peluso, J.J., Liu, X., Saunders, M.M., Claffey, K.P., Phoenix, K., 2008. Regulation of ovarian cancer cell viability and sensitivity to cisplatin by progesterone receptor membrane component-1. J. Clin. Endocrinol. Metabol. 93, 1592–1599.

Peluso, J.J., Griffin, D., Liu, X., Horne, M., 2014. Progesterone receptor membrane component-1 (PGRMC1) and PGRMC-2 interact to suppress entry into the cell cycle in spontaneously immortalized rat granulosa cells. Biol. Reprod. 91 (104), 101–112.

Ran A., F., Hsu D., P., Wright, J., Agarwala, V., Scott A., D., Zhang, F., 2013. Genome engineering using the CRISPR-Cas9 system. Nat. Protoc. 8, 2281–2308. https://doi.org/10.1038/nprot.2013.143.

Rohe, H.J., Ahmed, I.S., Twist, K.E., Craven, R.J., 2009. PGRMC1 (progesterone receptor membrane component 1): a targetable protein with multiple functions in steroid signaling, P450 activation and drug binding. Pharmacol. Ther. 121, 14–19.

Selman, K., Wallace, R.A., Sarka, A., Qi, X., 1993. Stages of oocyte development in the zebrafish, Brachydanio rerio. J. Morphol. 218, 203–224.

Szczesna-Skorupa, E., Kemper, B., 2011. Progesterone receptor membrane component 1 inhibits the activity of drug-metabolizing cytochromes P450 and binds to cytochrome P450 reductase. Mol. Pharmacol. 79, 340–350.

Thomas, P., 2008. Characteristics of membrane progestin receptor alpha (mPRα) and progesterone membrane receptor component 1 (PGMRC1) and their roles in mediating rapid progestin actions. Front. Neuroendocrinol. 29, 292–312.

Thomas, P., Pang, Y., Dong, J., Groenen, P., Kelder, J., de Vlieg, J., Zhu, Y., Tubbs, C., 2007. Steroid and G protein binding characteristics of the seatrout and human progestin membrane receptor α subtypes and their evolutionary origins. Endocrinology 148, 705–718.

Thomas, P., Pang, Y., Dong, J., 2014. Enhancement of cell surface expression and receptor functions of membrane progestin receptor α (mPRα) by progesterone receptor membrane component 1 (PGRMC1): evidence for a role of PGRMC1 as an adaptor protein for steroid receptors. Endocrinology 155, 1107–1119.

Tyler, C., Sumpter, J., 1996. Oocyte growth and development in teleosts. Rev. Fish Biol. Fish. 6, 287–318.

Wu, X.J., Thomas, P., Zhu, Y., 2018. Pgrmc1 knockout impairs oocyte maturation in zebrafish. Front. Endocrinol. 9, 560.

Zhang, Z., Lau, S.-W., Zhang, L., Ge, W., 2015. Disruption of zebrafish follicle-stimulating hormone receptor (fshr) but not luteinizing hormone receptor (lhcgr) gene by TALEN leads to failed follicle activation in females followed by sexual reversal to males. Endocrinology 156, 3747–3762.

Zhu, Y., Hanna, R.N., Schaaf, M.J., Spaink, H.P., Thomas, P., 2008. Candidates for membrane progestin receptors—past approaches and future challenges. Comp. Biochem. Physiol. C: Toxicol. Pharmacol. 148, 381–389.

Zhu, Y., Liu, D., Shaner, Z.C., Chen, S., Hong, W., Stellwag, E.J., 2015. Nuclear progestin receptor (pgr) knockouts in zebrafish demonstrate role for pgr in ovulation but not in rapid non-genomic steroid mediated meiosis resumption. Front. Endocrinol. 6, 37.